

Irregular Traffic Time Series Forecasting Based on Asynchronous Spatio-Temporal Graph Convolutional Network

Weijia Zhang¹, Le Zhang², Jindong Han³, Hao Liu^{1,3}, Jingbo Zhou², Yu Mei², Hui Xiong^{1,3}

¹The Hong Kong University of Science and Technology (Guangzhou),

²Baidu Inc., ³The Hong Kong University of Science and Technology

wzhang411@connect.hkust-gz.edu.cn, {zhangle09, zhoujingbo, meiyu}@baidu.com,

jhanao@connect.ust.hk, {liuh, xionghui}@ust.hk

ABSTRACT

Accurate traffic forecasting at intersections governed by intelligent traffic signals is critical for the advancement of an effective intelligent traffic signal control system. Indeed, it not only helps optimize traffic signal control strategies to improve traffic efficiency, but also enables autonomous vehicles to make safe and efficient routing and navigation decisions with foresight. However, due to the irregular traffic time series produced by intelligent intersections, the traffic forecasting task becomes much more intractable and imposes three major new challenges: 1) asynchronous spatial dependency, 2) irregular temporal dependency among traffic data, and 3) variable-length sequence to be predicted, which severely impede the performance of current traffic forecasting methods. To this end, we propose an **Asynchronous Spatio-tEmporal graph convolutional nEtwoRk (ASEER)** to predict the traffic states of the lanes entering intelligent intersections in a future time window. Specifically, by linking lanes via a traffic diffusion graph, we first propose an **Asynchronous Graph Diffusion Network** to model the asynchronous spatial dependency between the time-misaligned traffic state measurements of lanes. After that, to capture the temporal dependency within irregular traffic state sequence, a learnable personalized time encoding is devised to embed the continuous time for each lane. Then we propose a **Transformable Time-aware Convolution Network** that learns meta-filters to derive time-aware convolution filters with transformable filter sizes for efficient temporal convolution on the irregular sequence. Furthermore, a **Semi-Autoregressive Prediction Network** consisting of a state evolution unit and a semi-autoregressive predictor is designed to effectively and efficiently predict variable-length traffic state sequences. Finally, extensive experiments on two real-world datasets demonstrate the effectiveness of ASEER compared with nine competitive baseline algorithms in six metrics.

1 INTRODUCTION

Intelligent Traffic Signal Control System (ITSCS) has emerged as an indispensable building block in facilitating autonomous driving [10]. With the help of Vehicle-to-Infrastructure (V2I) communication technologies, ITSCS can provide important information to autonomous vehicles about the state of traffic signals and the surrounding traffic environment [17]. Particularly, it is a critical capability of ITSCS to forecast the traffic dynamics of the intersections controlled by intelligent traffic signals. An accurate traffic forecasting for intelligent intersections provides the foundation for autonomous vehicles to make foresighted routing and navigation decisions, with the objective of safe and efficient autonomous driving. Additionally, it facilitates the optimization of traffic signal

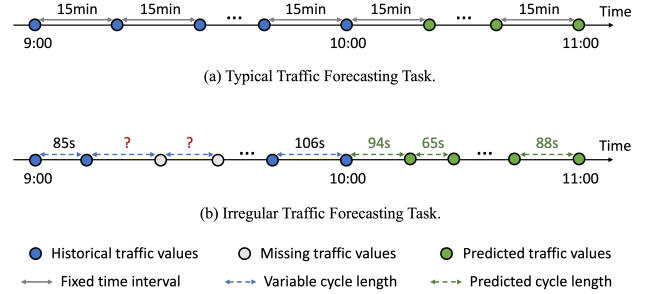


Figure 1: An illustrative example of traffic forecasting for the future one hour (10:00-11:00) based on traffic data in the past one hour (9:00-10:00). (a) Typical traffic forecasting task predicts a fixed-length sequence of traffic values (e.g., flow) in the future time window based on complete historical traffic value sequences with fixed time intervals. (b) Irregular traffic forecasting task aims to predict a variable-length sequence of traffic states (i.e., traffic signal cycle length and the corresponding traffic flow) in the future time window based on incomplete historical traffic state sequences with variable time intervals.

control strategies to reduce traffic congestion and improve traffic throughput, thereby contributing to the establishment of an efficient and smooth transportation system.

However, traffic forecasting at intelligent intersections (*a.k.a.* irregular traffic forecasting) is significantly different from previous traffic forecasting tasks that typically predict traffic values (e.g., flow, speed) on highways for a fixed time interval (e.g., 15 minutes) [18, 33, 35]. On the one hand, the intelligent traffic signal adaptively adjusts its cycle length to adapt to traffic flow changes at the intersection [31]. On the other hand, traffic flows crossing the intersection are dynamically regulated by adaptive signal control strategies with varying cycle lengths. As a result, the traffic states in intelligent intersections can consist of both the traffic signal cycle lengths and the corresponding traffic flows during these cycles, which are entangled and influenced by each other, rendering the traffic dynamics in intelligent intersections more complicated. Furthermore, as the traffic signal cycle lengths can significantly vary across both time and intersections, traffic state sequences produced by intelligent intersections exhibit considerable irregular and time-misaligned characteristics. Figure 1 shows an illustration of distinction between the typical traffic forecasting task and irregular traffic forecasting task. In this illustrative example, the objective is to forecast traffic patterns for the next hour according to the past hour’s traffic data. Typical traffic forecasting task predicts a

fixed-length sequence of traffic values (e.g., flow) in the future time window based on complete historical traffic value sequences with fixed time intervals. In contrast, our irregular traffic forecasting task aims to predict a variable-length sequence of traffic states, including traffic signal cycle lengths and the corresponding traffic flows, in the future time window based on incomplete historical traffic state sequences characterized by variable time intervals.

It is a non-trivial task for irregular traffic forecasting, which faces the following three major challenges: (1) *Asynchronous spatial dependency*. Traffic flow has obvious spatial dependency due to its diffusion nature in the road network [18]. However, the traffic signals at different intersections usually have distinct cycle beginning times and lengths because of the distinctions in traffic conditions and control strategies. As a result, the traffic state measurements of different lanes cannot be aligned at times, causing asynchronism in spatial dependency modeling. Furthermore, the data missing issue will exacerbate such spatial asynchronism, which hinders the direct application of established spatial dependency modeling techniques for typical traffic forecasting tasks [18, 35]. Thus, the first challenge is how to model the asynchronous spatial dependency between time-misaligned traffic state measurements. (2) *Irregular temporal dependency*. The future traffic states of each lane are correlated with its historical traffic states. Different from prior traffic forecasting studies [18, 35] that process a regular traffic time series, we face an irregular traffic state sequence with alterable time intervals between two successive measurements. Such time interval irregularity can come from varying signal cycle lengths and data missing issue in the measurement of sensors. It leads to irregularity in temporal dependency modeling, thus prior traffic forecasting methods are uncompetitive in handling it. Therefore, the second challenge is how to capture the irregular temporal dependency within traffic state sequences. (3) *Variable-length sequence to be predicted*. Our goal is to predict the complete traffic state sequences in a future time window (e.g., the next hour). However, with the signal cycle lengths varying at different intersections and times, the sequence lengths to be predicted are usually variable as well. An autoregressive prediction model is plausible for variable-length sequence prediction, whereas the predicted sequence could be long, which results in such an approach suffering from severe error accumulation and poor prediction efficiency issues [21, 22]. How to effectively and efficiently predict variable-length traffic state sequences is the last challenge.

To tackle the above challenges, we present an **Asynchronous Spatio-tEmporal graph convolutional nEtwoRk (ASEER)** for irregular traffic forecasting. Specifically, we first formulate a traffic diffusion graph by representing lanes as nodes and constructing edges in terms of geographical proximity and lane-level road network reachability. Next, we propose an Asynchronous Graph Diffusion Network to model the asynchronous spatial dependency between the time-misaligned traffic state measurements of nodes based on the graph. It allows each node to asynchronously diffuse its traffic state measurement to its neighbors, which receive and store the traffic state in their message buffers. The node then performs an asynchronous graph convolution to attain spatial representation of the measurement by attentively integrating the stored traffic messages. After that, to capture the temporal dependency within irregular traffic state sequences, a learnable personalized time encoding

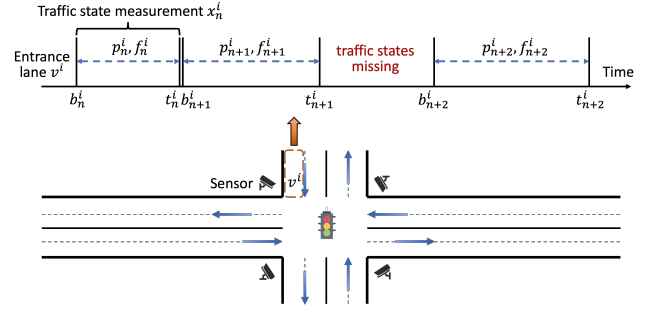


Figure 2: An illustration of traffic states measured from an entrance lane at an intelligent intersection.

is first devised to embed the continuous times of each node’s traffic measurements. Then we propose a Transformable Time-aware Convolution Network that learns meta-filters to derive time-aware convolution filters with transformable filter sizes based on the obtained spatial representations and traffic state measurements along with the time encoding. The derived time-aware convolution filters are applied for efficient temporal convolution on the irregular sequences to acquire the spatiotemporal representation for each node. Finally, we design a Semi-Autoregressive Prediction Network to iteratively predict variable-length traffic state sequences in an effective and efficient way. In each prediction step, a state evolution unit, whose hidden state is initialized by the spatiotemporal representation, is introduced to evolve each node’s traffic hidden state with the elapsed time, and a semi-autoregressive predictor is adopted to predict a sequence of consecutive traffic states based on the evolutionary, initial traffic hidden states, and the predicted elapsed time.

Our major contributions can be summarized as follows:

- We investigate a new Irregular Traffic Forecasting problem, which imposes three new significant challenges for traffic forecasting from spatial, temporal, and sequence prediction perspectives.
- We propose an Asynchronous Graph Diffusion Network to model the asynchronous spatial dependency among time-misaligned traffic data.
- We propose a Transformable Time-aware Convolution Network with personalized time encoding to efficiently capture temporal dependency within irregular traffic sequences.
- We design a Semi-Autoregressive Prediction Network to empower effective and efficient prediction for variable-length traffic state sequences.
- Extensive experiments on two real-world datasets demonstrate the superiority of ASEER compared with nine competitive baselines in six metrics.

2 PRELIMINARIES

Considering a set of N entrance lanes $\mathbf{V} = \{v^1, v^2, \dots, v^N\}$ directly connect with multiple intersections, where each lane collects its real-time traffic data via the deployed sensor.

DEFINITION 1 (TRAFFIC STATE MEASUREMENT). *As illustrated in Figure 2, the n -th chronological traffic state measurement*

of a lane v^i is defined as $x_n^i = \langle p_n^i, f_n^i \rangle \in \mathbf{X}$, where p_n^i denotes the traffic signal cycle length of this measurement in the intersection that v^i connects, and f_n^i is the traffic flow in v^i during this signal cycle. We further define b_n^i and t_n^i as the beginning and end timestamps (in second) of this cycle, and we have $t_n^i = b_n^i + p_n^i - 1$. As traffic signal cycles occur consecutively in real-world scenarios, there is $b_{n+1}^i = t_n^i + 1$ in the absence of any missing traffic states between x_n^i and x_{n+1}^i .

Note that due to the unpredictable systematic failures of sensors, there could be multiple traffic states missing between two successive observed measurements. Our problem is defined below.

PROBLEM 1 (IRREGULAR TRAFFIC FORECASTING). Given a historical time window \mathcal{T} , e.g., one hour, before current timestamp t , and a set of historical traffic state measurements $\mathbf{X}_{[t-\mathcal{T}:t]}$ of all lanes \mathbf{V} obtained during \mathcal{T} , our problem is to predict the complete traffic states $\widehat{\mathbf{X}}_{[t+1:t+\tau]}$ for all lanes in the next τ time window, e.g., the next hour, formalized as:

$$\mathcal{F}(\mathbf{X}_{[t-\mathcal{T}:t]}) \longrightarrow \widehat{\mathbf{X}}_{[t+1:t+\tau]}, \quad (1)$$

where $\mathcal{F}(\cdot)$ is the prediction model we aim to learn.

3 METHODOLOGY

3.1 Framework Overview

Figure 3 shows the framework overview of ASEER, which consists of three major components. Specifically, Asynchronous Graph Diffusion Network (AGDN) models asynchronous spatial dependency based on a traffic diffusion graph, where nodes are represented by lanes and edges are constructed via the geographical proximity and lane-level road network reachability between lanes. When a node has a traffic state measurement, AGDN asynchronously diffuses the node's traffic measurement to its neighbors, which receive and store the diffused traffic state into their message buffers. Next, the node performs an asynchronous graph convolution by attentively integrating the stored traffic messages, and then the buffer will be cleared. After that, a Transformable Time-aware Convolution Network (TTCN) is adopted to model the temporal dependency within irregular traffic state sequences. TTCN learns meta-filters to derive time-aware convolution filters with transformable filter sizes based on traffic states' spatial representations obtained from AGDN and traffic measurements along with personalized time encoding. Then the derived time-aware convolution filters are applied for efficient temporal convolution on irregular traffic state sequences to acquire the spatiotemporal representation for each node. Finally, a Semi-Autoregressive Prediction Network (SAPN) is devised to iteratively predict variable-length traffic state sequences. In each prediction step, a State Evolution Unit (SEU), whose hidden state is initialized by spatiotemporal representations, is first introduced to evolve each node's future traffic hidden state with the elapsed time, then a Semi-Autoregressive Predictor (SAP) is adopted to predict a sequence of consecutive traffic states based on both evolutionary, initial traffic hidden states, and predicted elapsed time.

3.2 Asynchronous Spatial Dependency Modeling

Previous traffic forecasting studies model spatial dependency by introducing graph neural networks to synchronously diffuse and

aggregate the time-aligned traffic state measurements between different sensor nodes [18, 35]. However, in our problem, the observed traffic state measurements of different lanes cannot be aligned due to the distinct timestamps of traffic signal cycles in different intersections and data missing issue, which causes severe asynchronism in modeling spatial dependency.

To this end, by linking lanes via a traffic diffusion graph, we propose an Asynchronous Graph Diffusion Network (AGDN) to model the asynchronous spatial dependency between the time-misaligned traffic measurements. The key idea of AGDN is that each node asynchronously diffuses its traffic state measurement to the adjacent nodes once it's observed. Then, the adjacent nodes receive and store traffic state from others into a message buffer of itself. Next, each node will integrate its stored traffic messages via an asynchronous graph convolution operation. We detail it below. **Diffusion Graph Construction.** To model spatial dependency between lanes' traffic dynamics, we construct a traffic diffusion graph $\mathcal{G} = (\mathcal{V}, \mathcal{X}_{\mathcal{V}}, \mathcal{E}, \mathcal{X}_{\mathcal{E}})$, where the graph nodes $\mathcal{V} = \mathbf{V}$ represents a set of lanes, $\mathcal{X}_{\mathcal{V}} = \mathbf{X}_{[t-\mathcal{T}:t]}$ denotes features of nodes \mathcal{V} , \mathcal{E} are a set of edges indicating proximity between nodes, and $\mathcal{X}_{\mathcal{E}}$ are features in edges \mathcal{E} . Specifically, we define proximity $e^{ij} \in \mathcal{E}$ between v^i and v^j as:

$$e^{ij} = \begin{cases} 1, & \text{if } \text{dist}(v^i, v^j) < \epsilon, i \neq j \\ 0, & \text{if } \text{otherwise} \end{cases}, \quad (2)$$

where $\text{dist}(v^i, v^j)$ denotes geographical distance [39] between node v^i and v^j , ϵ is a threshold, and there is no self-loop for each node. We also define some edge features $x_e^{ij} \in \mathcal{X}_{\mathcal{E}}$ between nodes v^i and v^j , including geographical distance and the direct reachability in the lane-level road network. Note that it's not limited to geographical proximity and reachability, other graph construction approaches can also be embraced.

Asynchronous Diffusion and Storage. Assume a traffic state measurement x_{n-}^j of node v^j is observed at timestamp t_{n-}^j , then v^j will diffuse x_{n-}^j as a traffic message to its adjacent nodes $v^i \in \mathcal{N}_j$ in terms of edges \mathcal{E} , which can be more formally denoted as:

$$\text{AsynDiff}\left(v^j \xrightarrow{x_{n-}^j} \{v^i : \forall v^i \in \mathcal{N}_j\}\right). \quad (3)$$

For each node $v^i \in \mathcal{N}_j$, it receives the traffic message x_{n-}^j and then stores it into its message buffer \mathcal{B}^i for later use:

$$\text{Store}\left(x_{n-}^j \longrightarrow \{\mathcal{B}^i : \forall v^i \in \mathcal{N}_j\}\right). \quad (4)$$

Since the timestamps of traffic state measurements are misaligned for different nodes, the traffic messages diffusion and storage processes perform in an asynchronous way.

Asynchronous Graph Convolution. An immediate problem is how to exploit traffic messages stored in the message buffer to enhance each node's spatial perception. We achieve this by enforcing each node v^i asynchronously integrates the traffic messages in its message buffer \mathcal{B}^i via an asynchronous graph convolution operation, which is performed once a traffic state measurement x_n^i is observed in node v^i .

Specifically, we first employ x_n^i to query the message buffer \mathcal{B}^i for the proximity weights computation with each traffic message

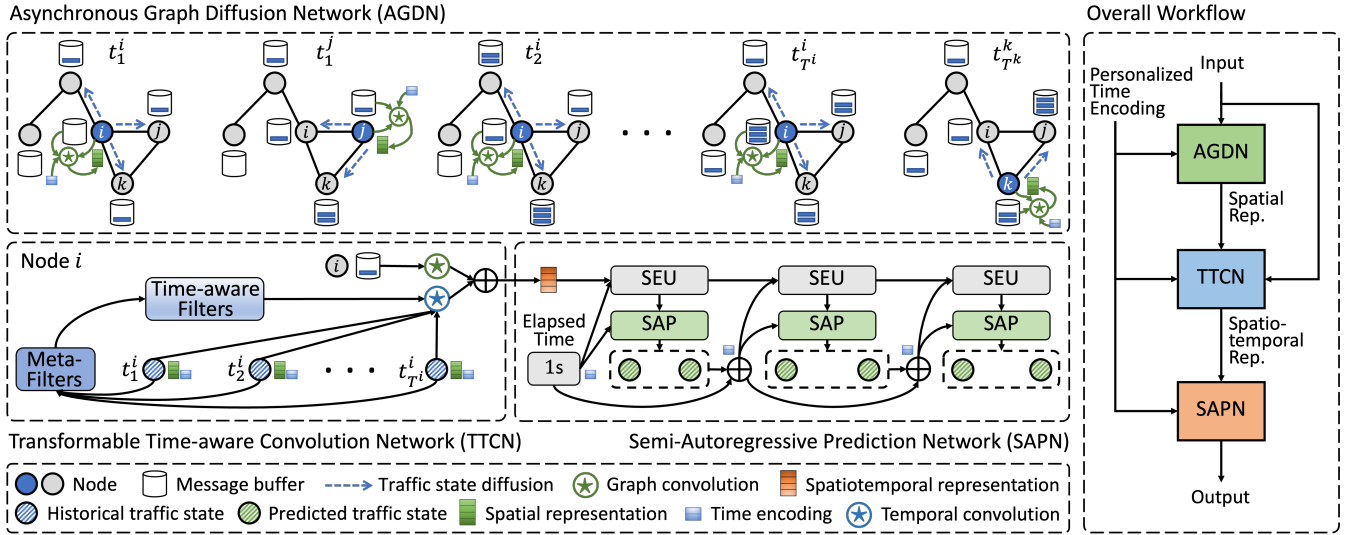


Figure 3: The framework overview of ASEER, which consists of three major components: Asynchronous Graph Diffusion Network (AGDN), Transformable Time-aware Convolution Network (TTCN), and Semi-Autoregressive Prediction Network (SAPN). The traffic states are first inputted to AGDN to obtain spatial representations, which are incorporated by TTCN to acquire the spatiotemporal representations. After that, SAPN predicts the variable-length traffic state sequence based on the spatiotemporal representations. Throughout the entire process, personalized time encoding is used to embed continuous time.

$x_{n-}^j \in \mathcal{B}^i$ via the following attention operation:

$$\alpha_{nn-} = \frac{\exp(\beta_{nn-})}{\sum_{x_{n-}^j \in \mathcal{B}^i} \exp(\beta_{nn-})}, \quad (5)$$

$$\beta_{nn-} = \mathbf{v}^\top \tanh(\mathbf{W}_a [x_n^i \oplus x_{n-}^j \oplus \phi^i(t_n^i - t_{n-}^j) \oplus x_e^{ij}]),$$

where \oplus indicates concatenation operation, \mathbf{v} and \mathbf{W}_a are learnable parameters, and $\phi^i(\cdot)$ is a learnable time encoding function to embed cycle-related patterns for each node that will be detailed in the next section.

Once the proximity weights are obtained, we asynchronously integrate node's stored traffic messages received from neighbors via an attentive graph convolution to obtain the spatial representation:

$$\tilde{h}_n^i = \text{MLP} \left(\sum_{x_{n-}^j \in \mathcal{B}^i} \alpha_{nn-} \cdot [x_{n-}^j \oplus \phi^i(t_n^i - t_{n-}^j) \oplus x_e^{ij}] \right), \quad (6)$$

where MLP represents a multi-layer perceptron. It's noteworthy that after each asynchronous graph convolution operation on \mathcal{B}^i , all the traffic messages in it will be cleared. It indicates that each node only integrates adjacent traffic messages from its last traffic measurement's timestamp to the current measurement's timestamp t_n^i , which guarantees each message is utilized exactly once to avoid redundant information and computation in asynchronous spatial dependency modeling.

Define $x_{T_i}^i$ as the last observed traffic state measurement of node v^i during historical time window \mathcal{T} . There could be some messages received and stored in the message buffer \mathcal{B}^i after the timestamp $t_{T_i}^i$ of this measurement. Thus, we perform a similar asynchronous graph convolution operation for these remaining

messages by adding a virtual measurement $\tilde{x}_{T_i}^i$ at timestamp $t_{T_i}^i$ without traffic state values. The obtained spatial representation is denoted as $\tilde{h}_{T_i}^i$.

3.3 Irregular Temporal Dependency Modeling

Convolutional Neural Network (CNN) [16] is widely applied to typical traffic forecasting tasks for its both efficiency and effectiveness in temporal dependency modeling [11, 15, 33, 35]. However, applying CNN to our task faces two problems. First, CNN fails to directly process irregular traffic sequences with variable sequence lengths. Second, CNN is incompetent to model temporal dependency in the sequence with varying time intervals, as its filter parameters are fixed and cannot adaptively adjust according to the varying time intervals between successive data points.

To tackle the above problems, we propose a Transformable Time-aware Convolution Network (TTCN) which learns a meta-filter to derive the time-aware convolution filter with transformable filter size so that enables to efficiently model temporal dependency in the irregular traffic state sequence, and further devise a personalized time encoding function to embed the unique cycle-related patterns for each node. Specifically, given the historical time window \mathcal{T} before t , for each node v^i , we first concatenate the traffic state measurement x_n^i during \mathcal{T} with the corresponding spatial representation \tilde{h}_n^i and the encoding of time intervals $\phi^i(t_{T_i}^i - t_n^i)$ from timestamp t_n^i to timestamp $t_{T_i}^i$ of the last traffic state measurement:

$$z_n^i = [x_n^i \oplus \tilde{h}_n^i \oplus \phi^i(t_{T_i}^i - t_n^i)]. \quad (7)$$

3.3.1 Personalized Time Encoding. The desired time encoding should not only indicate the absolute time interval but also imply

the unique cycle-related patterns of traffic dynamics in different nodes. For example, a time interval may signify a distinct number of traffic signal cycles for different intersections, which is important for temporal dependency modeling, especially when the time interval spans multiple missing traffic states. Inspired by the positional encoding in transformer [29], we introduce a personalized time encoding by adopting a learnable trigonometric function to embed the time interval Δt for each node:

$$\phi_p^i(\Delta t)[s] = \begin{cases} \Delta t, & \text{if } s = 0 \\ \sin(\omega_k^i \Delta t), & \text{if } s = 2k + 1 \\ \cos(\omega_k^i \Delta t), & \text{if } s = 2k + 2 \end{cases}, \quad (8)$$

where the above equation denotes s -th element of the time encoding $\phi_p^i(\Delta t) \in \mathbb{R}^{d_{\phi}+1}$, and ω_k^i are learnable parameters to indicate the cyclical characteristics of this function. Each node has an individual time encoding function with separate parameters so that can learn its unique cycle-related patterns.

Due to the data missing problem, some nodes may have too sparse measurement data to learn a satisfactory unique time encoding function. Hence, we also jointly learn a generic time encoding $\phi_g(\Delta t)$, which has a similar function expression to Eq. (8) but is shared by all nodes. Then, we introduce a learnable weight λ_i for each node to adaptively integrate the above two time encoding:

$$\phi^i(\Delta t) = (1 - \exp(-\lambda_i^2)) \cdot \phi_p^i(\Delta t) + \exp(-\lambda_i^2) \cdot \phi_g(\Delta t). \quad (9)$$

λ_i is initialized to be close to zero so that the nodes with limited or even no available data can weigh more on generic time encoding.

3.3.2 Transformable Time-aware Convolution Network. In this section, we assume all the following operations are performed on node v^i , thus we omit the superscript i to ease the presentation. We first define $Z_{t-\mathcal{T}+1:t} = \{z_1, \dots, z_T\}$ and T as the sequence length of $Z_{t-\mathcal{T}+1:t}$. Then we leverage a meta-filter to derive the time-aware convolution filter with dynamic parameters and transformable filter size T based on sequence inputs, formulated as:

$$\mathbf{f}_d = [\text{Norm}(\mathbf{F}_d(z_1)), \dots, \text{Norm}(\mathbf{F}_d(z_T))], \quad (10)$$

$$\text{Norm}(\mathbf{F}_d(z_n)) = \frac{\exp(\mathbf{F}_d(z_n))}{\sum_{z_{n'} \in Z_{t-\mathcal{T}+1:t}} \exp(\mathbf{F}_d(z_{n'}))},$$

where $\mathbf{f}_d \in \mathbb{R}^{T \times D_{im}}$ is the derived filter for d -th feature map, and \mathbf{F}_d denotes the meta-filter that can be instantiated by learnable neural networks. We normalize the derived filter parameters along the temporal dimension to ensure consistent scaling of the convolution results for variable-length sequences.

With D filters derived according to Eq. (10), we obtain the traffic sequence representation $h_T \in \mathbb{R}^D$ via the following temporal convolution operation:

$$h_T = [Z_{t-\mathcal{T}+1:t} \star \mathbf{f}_1, \dots, Z_{t-\mathcal{T}+1:t} \star \mathbf{f}_D], \quad (11)$$

$$Z_{t-\mathcal{T}+1:t} \star \mathbf{f}_d = \sum_{n=1}^T \mathbf{f}_d[n]^\top Z_{t-\mathcal{T}+1:t}[n],$$

where \star denotes the convolution operation. Then we attain the overall spatiotemporal representation for each node via the following representations integration:

$$\mathcal{H}_T = h_T + \bar{h}_T. \quad (12)$$

Compared to CNN, TTCN has several advantages in modeling sequence's temporal dependency with irregular time intervals. First, the derived filter is transformable according to sequence length, which enables it to adaptively process variable-length sequences. Moreover, it can derive tailored parameterized filters for sequences with varying time intervals or other characteristics. It is worth noting that as the learnable parameters of meta-filter are independent of sequence length, TTCN is allowed to directly model the long-term temporal dependency through an arbitrarily large-size convolution filter without increasing any filter parameters.

3.4 Traffic State Sequence Prediction

Our goal is to predict the complete traffic state sequences, including a sequence of traffic signal cycle lengths and the corresponding traffic flows, for all nodes in a future time window. However, the sequences to be predicted have variable lengths in terms of the differences in intersections, time windows, or prediction algorithms, and the sequence lengths cannot be known in advance. An autoregressive prediction model iteratively predicts the next step's value based on previously predicted values, which seems feasible for the variable-length sequence prediction. However, the requirements for long sequence prediction can lead to severe error accumulation and poor prediction efficiency issues in the autoregressive approaches [21, 22].

To tackle the above problems, we design a Semi-Autoregressive Prediction Network (SAPN) to predict the traffic state sequence. SAPN consists of a state evolution unit to evolve each node's traffic hidden state with the elapsed time and a semi-autoregressive predictor to predict a sequence of consecutive traffic states in each prediction step. SAPN iteratively predicts sub-sequences until the complete sequence meets the requirements of the task, which not only enables variable-length sequence prediction in an efficient way but also mitigates the error accumulation issue for long sequence prediction. Since prediction processes are the same for all nodes, we omit the superscript i to ease the presentation as well.

To be specific, we employ the spatiotemporal representation \mathcal{H}_T acquired from AGDN and TTCN as the initial traffic hidden state. In each prediction step, a semi-autoregressive predictor predicts a sequence of consecutive traffic states based on the evolutionary and initial traffic hidden states, as well as the predicted elapsed time encoding, formulated as:

$$\hat{x}_{T+m\xi+1:T+(m+1)\xi} = \text{SAP} \left(\left[\hat{\mathcal{H}}_{T+m\xi+1} \oplus \mathcal{H}_T \oplus \phi(\hat{\delta}_{T+m\xi+1}) \right] \right), \quad (13)$$

$$\left[\hat{p}_{T+m\xi+1:T+(m+1)\xi}, \hat{u}_{T+m\xi+1:T+(m+1)\xi} \right] = \hat{x}_{T+m\xi+1:T+(m+1)\xi},$$

where ξ is the prediction step size, $m \geq 0$ denotes m -th prediction step, $\hat{p}_{T+m\xi+1:T+(m+1)\xi}$ and $\hat{u}_{T+m\xi+1:T+(m+1)\xi}$ respectively represents a sequence of consecutive cycle lengths and unit time traffic flows from index $T + m\xi + 1$ to $T + (m + 1)\xi$, and $\hat{\delta}_{T+m\xi+1}$ indicates the elapsed time over the timestamp t_T of sequence's last observed measurement. $\hat{\delta}_{T+m\xi+1}$ is initialized to 1 when $m = 0$, and iteratively updates based on the accumulation of predicted cycle lengths:

$$\hat{\delta}_{T+(m+1)\xi+1} = \hat{\delta}_{T+m\xi+1} + \sum_{k=1}^{\xi} \hat{p}_{T+m\xi+k}. \quad (14)$$

Since the underlying traffic state is actually dynamically evolving with passage of time, we introduce a state evolution unit to learn to evolve each node's traffic hidden state with the elapsed time:

$$\widehat{\mathcal{H}}_{T+m\xi+1} = \text{SEU} \left(\widehat{\mathcal{H}}_{T+(m-1)\xi+1}, \phi(\hat{\sigma}_{T+(m-1)\xi+1}) \right), \quad (15)$$

where $\hat{\sigma}_{T+(m-1)\xi+1} = 1$ and $\widehat{\mathcal{H}}_{T+(m-1)\xi+1} = \mathcal{H}_T$ if $m = 0$, otherwise $\hat{\sigma}_{T+(m-1)\xi+1} = \sum_{k=1}^{\xi} \hat{p}_{T+(m-1)\xi+k}$. Next, we can obtain the corresponding traffic flows of predicted traffic signal cycles by multiplying the predicted unit time traffic flows with cycle lengths:

$$\hat{J}_{T+m\xi+1:T+(m+1)\xi} = \hat{u}_{T+m\xi+1:T+(m+1)\xi} \odot \hat{P}_{T+m\xi+1:T+(m+1)\xi}, \quad (16)$$

where \odot denotes Hadamard product. By iteratively performing the above prediction step until the predicted sequence covers the required time window, we can derive the variable-length traffic state sequence we expect.

Compared to autoregressive models, our SAPN predicts a variable-length sequence with fewer prediction steps, which improves prediction efficiency and may reduce the risks of causing prediction error accumulation. It's not hard to see that both the autoregressive and non-autoregressive prediction models can be regarded as a special case of semi-autoregressive model when the prediction step size is set to one or the length of sequence. Thus, our SAPN can also be considered as incorporating both strengths of autoregressive and non-autoregressive prediction models to predict variable-length sequences. In the implementation, we instantiate SAP via MLP and SEU via Gated Recurrent Unit [7].

3.5 Model Training

Due to the data missing problem, we design three masked losses to train our model. The first loss is introduced to optimize the traffic signal cycle length forecasting via the masked Mean Absolute Error (MAE):

$$\mathcal{L}_p = \frac{1}{N \times L_{\perp}^i} \sum_{i=1}^N \sum_{l=1}^{L^i} \left| \hat{p}_{T^i+l}^i - p_{T^i+l}^i \right| \times \zeta_{T^i+l}^i, \quad (17)$$

where T^i is the length of the historical measurement sequence of node v^i and L^i is the length of the ground truth traffic state sequence of v^i . $\zeta_{T^i+l}^i$ is a mask item, which equals zero if the ground truth value $p_{T^i+l}^i$ is missing, otherwise it equals one, and L_{\perp}^i denotes the number of nonzero mask items for each node.

To further mitigate the error accumulation in traffic signal cycle lengths prediction, we additionally introduce a timing loss to improve the accuracy of the predicted elapsed time accumulated by cycle lengths:

$$\mathcal{L}_{\delta} = \frac{1}{N \times L_{\perp}^i} \sum_{i=1}^N \sum_{l=1}^{L^i} \left| \hat{\delta}_{T^i+l}^i - \delta_{T^i+l}^i \right| \times \zeta_{T^i+l}^i. \quad (18)$$

Similarly, we introduce a masked MAE loss to optimize the corresponding traffic flow prediction for each traffic signal cycle:

$$\mathcal{L}_f = \frac{1}{N \times L_{\perp}^i} \sum_{i=1}^N \sum_{l=1}^{L^i} \left| \hat{u}_{T^i+l}^i \times p_{T^i+l}^i - f_{T^i+l}^i \right| \times \zeta_{T^i+l}^i. \quad (19)$$

Since traffic flow prediction is also based on cycle lengths, to avoid disturbance from the error of predicted cycle lengths, we use the

ground truth cycle lengths to calculate the corresponding traffic flows in the training phase.

Consequently, ASEER aims to jointly minimize an overall objective that combines the above three masked losses:

$$\mathcal{L} = \mathcal{L}_p + \mathcal{L}_{\delta} + \mathcal{L}_f. \quad (20)$$

3.6 Complexity Analysis

In this section, we analyze the time complexity of ASEER. Given the historical and predicted time windows, we let T^i , M^i , \mathcal{N}_i denote the number of historical traffic state measurements, total prediction steps, and neighbors of node v^i , denote N as the number of nodes, ξ as prediction step size, and let d denote the dimensions for all feature representation vectors to ease the presentation.

The time complexity of AGDN module is mainly determined by processing all the traffic messages stored in the buffers. Each node diffuses its traffic state measurements to its neighbors, and the nodes would clear their buffers after performing asynchronous graph convolution on the stored traffic messages (*i.e.*, a message would be computed only once), thus each node v^i would lead to $T^i \mathcal{N}_i$ messages for computation. Therefore, the time complexity of AGDN module would be $O(\sum_{i=1}^N T^i \mathcal{N}_i d^2)$.

For the TTCN module, the time complexity is mainly from generating time-aware convolution filters, where a $T^i \times d$ dimensional filter incurs a cost of $O(T^i d^2)$. We generate d filters, thus we obtain the time complexity for TTCN module as $O(\sum_{i=1}^N T^i d^3)$.

For the SAPN module, as each prediction step incurs a cost of $O(d^2 + d\xi)$, the time complexity of M^i prediction steps for all nodes would be $O(\sum_{i=1}^N M^i (d^2 + d\xi))$.

The time complexity of generating personalized time encoding for a continuous time is $O(d)$, which is a lower-order term when considering the time complexity of each module, and thus can be neglected. Hence, we deduce the overall time complexity of ASEER:

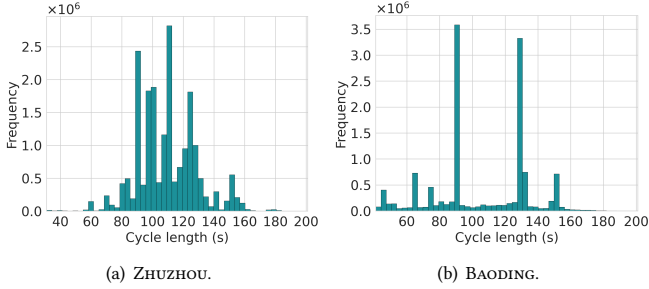
$$O \left(\sum_{i=1}^N \left(T^i d^2 (\mathcal{N}_i + d) + M^i (d^2 + d\xi) \right) \right). \quad (21)$$

Fortunately, the time complexity can be further reduced in practical real-time traffic forecasting applications. This is attributed to our model's character that the spatial representations acquired from AGDN can be asynchronously computed once the corresponding historical traffic measurements are observed. Assuming a traffic forecasting request is occurring at timestamp t , almost all spatial representations during the historical time window \mathcal{T} have been obtained. We only need to re-compute the spatial representations \tilde{h}_1^i and $\tilde{h}_{T^i}^i$ for the first chronological measurement and the remaining messages, inducing a time complexity $O(\sum_{i=1}^N (|\mathcal{B}_1^i| + |\mathcal{B}_r^i|) d^2)$, where $|\mathcal{B}_1^i|$ and $|\mathcal{B}_r^i|$ denotes the number of stored messages for the computation of \tilde{h}_1^i and $\tilde{h}_{T^i}^i$. Moreover, if we restrict to selecting a maximum of K messages (*e.g.*, the latest K messages) from these two buffers for computation, the time complexity can be further optimized to $O(\sum_{i=1}^N (\text{Min}(|\mathcal{B}_1^i|, K) + \text{Min}(|\mathcal{B}_r^i|, K)) d^2)$. Consequently, the practical time complexity of ASEER is reduced to:

$$O \left(\sum_{i=1}^N \left((\text{Min}(|\mathcal{B}_1^i|, K) + \text{Min}(|\mathcal{B}_r^i|, K)) d^2 + T^i d^3 + M^i (d^2 + d\xi) \right) \right). \quad (22)$$

Table 1: Statistics of datasets.

Description	ZHUZHOU	BAODING
# of measurements	19,824,504	13,093,975
# of sensors	620	264
Time range	2022/07/20-2022/10/02	2021/12/01-2022/02/25
Missing period ratio	44.2%	27.2%
Average / maximal ground truth sequence length to be predicted	57 / 213	64 / 155


Figure 4: Overall distributions of traffic signal cycle lengths.

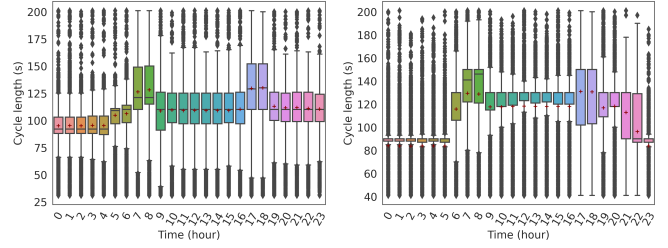
We verify the efficiency of ASEER and its components in Section 4.8.

4 EXPERIMENTS

4.1 Data Description and Analysis

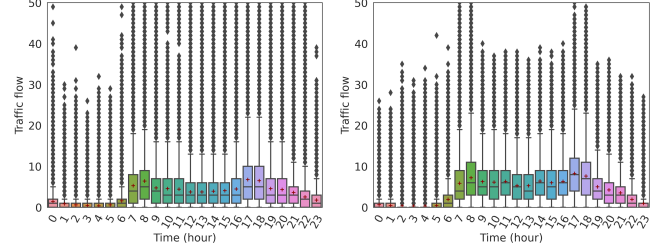
4.1.1 Datasets Description. We conduct experiments on two real-world datasets, ZHUZHOU and BAODING, which represent two major pilot cities of ITSCS and autonomous driving in China. Both datasets consist of a set of entrance lanes connecting to multiple intelligent intersections and large-scale traffic state measurements of lanes collected by the installed camera sensors. The statistics of the datasets are summarized in Table 1. Specifically, there are total 19,824,504 and 13,093,975 traffic state measurements on ZHUZHOU and BAODING, and the missing period ratios of the two datasets are 44.2% and 27.2%, respectively. Each measurement includes information about the beginning and end timestamps and cycle length of the traffic signal cycle, as well as the lane’s traffic flow during the signal cycle. Besides, ZHUZHOU has 620 lanes with sensors and ranges from July 20, 2022 to October 2, 2022. BAODING has 264 lanes with sensors and ranges from December 1, 2021 to February 25, 2022. The average, maximal ground truth sequence length to be predicted for the future one hour is 57, 213 on ZHUZHOU, and 64, 155 on BAODING. For both datasets, we aim to use the traffic state measurements in a fixed time window to predict the next time window. Thus, we take the data from the first 60% of the entire time slot as the training set, the following 20% for validation, and the remaining 20% as the test set. We calculate spherical distance as geographical distance and obtain reachability between lanes based on the lane-level road network.

4.1.2 Analysis on Datasets. The overall distributions of traffic signal cycle lengths on two datasets are depicted in Figure 4, where we can observe the cycle lengths can significantly vary from around



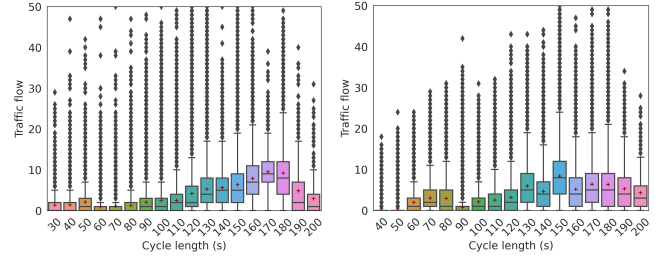
(a) Cycle lengths on ZHUZHOU.

(b) Cycle lengths on BAODING.



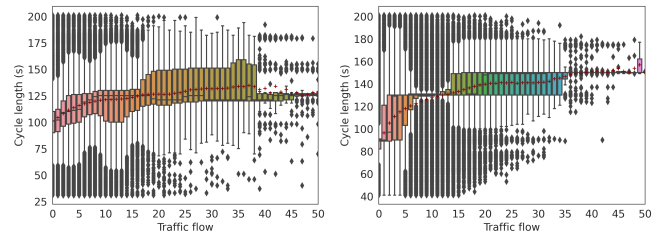
(c) Traffic flows on ZHUZHOU.

(d) Traffic flows on BAODING.

Figure 5: Temporal distributions of traffic signal cycle lengths and traffic flows across time. '+' denotes mean of the box plot.


(a) Distributions of traffic flows across dif-

(b) Distributions of traffic flows across dif-



(c) Distributions of cycle lengths across dis-

(d) Distributions of cycle lengths across dis-

Figure 6: Correlations between traffic flow and traffic signal cycle length. '+' denotes mean of the box plot.

40 to 200 seconds on both datasets, and BAODING has a denser cycle length distribution than ZHUZHOU.

Besides, Figure 5 illustrates temporal distributions of traffic signal cycle lengths and traffic flows across different hours on both datasets. We can observe cycle length and traffic flow consistently exhibit higher values during the daytime periods compared to

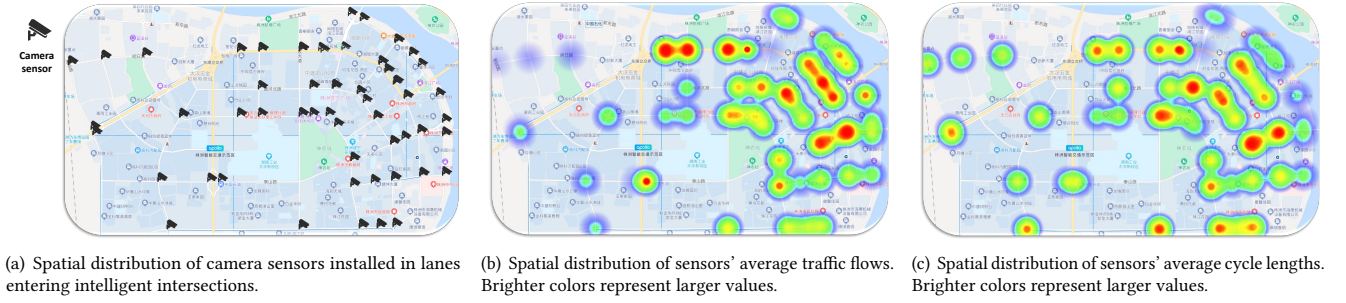


Figure 7: Spatial distributions of camera sensors and corresponding average traffic flows and cycle lengths on ZHUZHOU.

overnight periods. Moreover, they display similar peak patterns during the morning and evening rush hours and tend to vary in a positively correlated manner.

To further investigate the correlations between these two traffic states, we illustrate the variations in traffic flow distributions across different cycle lengths and vice versa in Figure 6. As can be seen in Figure 6(a) and Figure 6(b), traffic flow maintains an upward trend at first along with the increase of cycle length. A similar positive correlation can also be observed in Figure 6(c) and Figure 6(d), which display the variations in cycle length distributions across distinct traffic flows. However, we notice that with a further increase in cycle length, traffic flow tends to decrease. A similar situation is also shown in Figure 6(c). This can be attributed to the fact that although a positive correlation is expected between traffic flow and cycle length for the same lane, the lanes with the longest cycle lengths may not necessarily correspond to the highest traffic flows due to different traffic conditions and signal control strategies among these lanes, and vice versa.

Additionally, Figure 7 displays the spatial distributions [38] of camera sensors and corresponding average traffic flows and cycle lengths on ZHUZHOU as a representative. It can be noticed that both traffic flows and cycle lengths exhibit remarked geographical proximity, indicating that neighboring sensors tend to have similar traffic states. This finding provides partial justification for the effectiveness of the spatial dependency modeling component, AGDN, in the irregular traffic forecasting task.

4.2 Implementation Details

All experiments are performed on a Linux server with 20-core Intel(R) Xeon(R) Gold 6148 CPU @ 2.40GHz and NVIDIA Tesla V100 GPU. We set both historical and predicted time window lengths \mathcal{T} and τ to one hour, and choose distance threshold $\epsilon = 1\text{km}$ and prediction step size $\xi = 12$. We adopt three layers MLPs for asynchronous graph convolution, semi-autoregressive predictor, and meta-filters. The dimension for time encoding is set to $d_\phi = 16$, and dimensions for convolution filters, state evolution unit, and hidden layers of the above MLPs are all set to 64. To reduce parameter magnitude, in the implementation, we individualize the last layer's parameters but share the other parameters of MLP for meta-filters. We employ Adam optimizer to train our model, set learning rate to 0.001. ASEER and all learnable baselines are trained with an early stop criterion if the loss doesn't decrease lower on the validation set over 10 epochs.

4.3 Evaluation Metrics

We define six metrics to comprehensively evaluate the forecasting performance of algorithms. To evaluate the accuracy of predicted traffic signal cycle lengths, we quantify the predicted errors of both the beginning timestamps and cycle lengths via masked Mean Absolute Error (MAE), Root Mean Squared Error (RMSE), and Mean Absolute Percentage Error (MAPE):

$$\begin{aligned} \text{C-MAE} &= \frac{1}{2 \times N \times K_{\perp}^i} \sum_{i=1}^N \sum_{k=1}^{K^i} \left(|\hat{b}_k^i - b_k^i| + |\hat{p}_k^i - p_k^i| \right) \times \zeta_k^i, \\ \text{C-RMSE} &= \sqrt{\frac{1}{2 \times N \times K_{\perp}^i} \sum_{i=1}^N \sum_{k=1}^{K^i} \left((\hat{b}_k^i - b_k^i)^2 + (\hat{p}_k^i - p_k^i)^2 \right) \times \zeta_k^i}, \\ \text{C-MAPE} &= \frac{100\%}{2 \times N \times K_{\perp}^i} \sum_{i=1}^N \sum_{k=1}^{K^i} \left(\frac{|\hat{b}_k^i - b_k^i|}{\delta_k^i} + \frac{|\hat{p}_k^i - p_k^i|}{p_k^i} \right) \times \zeta_k^i. \end{aligned} \quad (23)$$

where K^i denotes the number of ground truth traffic states of each lane for evaluation, K_{\perp}^i is the number of observed measurements.

Since traffic flows depend on the corresponding traffic signal cycles, it's incomparable between the predicted and ground truth traffic flows if they are misaligned in signal cycles. Thus, we introduce two types of metrics to evaluate the prediction accuracy of traffic flows from multiple aspects. First, we assume all the traffic signal cycle lengths can be accurately predicted and use the ground truth cycle lengths for calculation, then we can directly compare the predicted and ground truth traffic flows via the following masked MAE and RMSE metrics:

$$\begin{aligned} \text{F-MAE} &= \frac{1}{N \times K_{\perp}^i} \sum_{i=1}^N \sum_{k=1}^{K^i} \left| \hat{f}_k^i - f_k^i \right| \times \zeta_k^i, \\ \text{F-RMSE} &= \sqrt{\frac{1}{N \times K_{\perp}^i} \sum_{i=1}^N \sum_{k=1}^{K^i} \left(\hat{f}_k^i - f_k^i \right)^2 \times \zeta_k^i}. \end{aligned} \quad (24)$$

Second, without the above assumption for cycle lengths, by computing traffic flow density at any timestamp, we calculate the masked Accumulative Absolute Error (AAE) between predicted and ground truth traffic flow density at identical timestamps:

$$\text{F-AAE} = \frac{1}{Z} \sum_{i=1}^N \sum_t \left| \hat{\rho}_t^i - \rho_t^i \right| \times \eta_t^i, \quad (25)$$

Table 2: Overall performance evaluated by C-MAE, C-RMSE, C-MAPE, F-MAE, F-RMSE, and F-AAE on ZHUZHOU and BAODING. The best-performing results are highlighted in bold.

Algorithm	ZHUZHOU						BAODING					
	C-MAE	C-RMSE	C-MAPE	F-MAE	F-RMSE	F-AAE	C-MAE	C-RMSE	C-MAPE	F-MAE	F-AAE	
LAST	50.5386	135.2616	5.54%	1.6669	3.0995	0.9192	42.8037	106.6547	4.79%	1.7521	2.8031	0.9557
HA	52.1532	135.3569	5.76%	1.4502	2.6567	0.7998	49.7496	114.8265	5.53%	1.5449	2.4594	0.8427
TCN	43.7838	110.1670	5.01%	1.3950	2.5824	0.7818	35.8318	95.7333	4.18%	1.3815	2.2060	0.7635
GRU	40.6209	99.8693	4.82%	1.3623	2.5553	0.7524	30.4621	83.4349	3.82%	1.3576	2.1655	0.7423
GRU-D	37.8531	84.6255	5.23%	1.3486	2.5333	0.7449	28.9117	82.5226	3.67%	1.3611	2.1735	0.7456
T-LSTM	39.1882	87.3458	5.38%	1.3641	2.5494	0.7539	29.0845	82.5219	3.76%	1.3673	2.1887	0.7475
DCRNN	38.5976	90.3190	4.36%	1.3318	2.4438	0.7348	31.0564	76.3693	3.86%	1.3681	2.1601	0.7467
GWNet	38.9913	106.6415	4.52%	1.3834	2.7915	0.7618	26.4988	84.3211	3.05%	1.3925	2.2482	0.7903
mTAND	37.5762	86.3045	3.93%	1.3563	2.5282	0.7498	27.2703	78.1066	2.86%	1.3575	2.1641	0.7487
ASEER	32.5803	72.1835	4.10%	1.2913	2.3864	0.7151	19.1188	54.4919	2.80%	1.3062	2.0827	0.7219

where $\hat{\rho}_t^i = \hat{f}_k^i / \hat{p}_k^i, t \in [\hat{b}_k^i, \hat{t}_k^i]$ and $\rho_t^i = f_k^i / p_k^i, t \in [b_k^i, t_k^i]$ are the predicted and ground truth traffic flow densities of lane v^i at timestamp t , respectively. η_t^i is the mask term at t , which equals one if ρ_t^i can be obtained from observed measurement, and zero otherwise. In our experiments, the timestamp is in seconds, and we use a normalization term Z to obtain the average result in minutes.

4.4 Baselines

We compare our approach with the following nine baselines. For fair comparison, all learnable baseline models are set to predict the unit time traffic flows like ASEER. In addition, except for autoregressive models (*i.e.*, GRU, GRU-D, T-LSTM, DCRNN), other baselines conduct prediction in a semi-autoregressive way with the same prediction step size as ASEER for better performance. We carefully tuned major hyper-parameters of each baseline based on their recommended settings for better performance on our datasets.

- **LAST** predicts future traffic states using each lane’s last historical traffic state measurement.
- **HA** predicts future traffic states using the average of each lane’s historical traffic state measurements.
- **TCN** [3] is the temporal convolutional network consisting of causal and dilated convolutions. We apply it to our datasets by padding or intercepting all the sequences to a fixed length. We stack 6 temporal convolution layers with filter size of 3.
- **GRU** [7] is a powerful variant of recurrent neural networks with a gated recurrent unit.
- **GRU-D** [5] improves GRU with a time-aware decay mechanism for irregular time series classification. We modify it to predict traffic states using a GRU-based decoder.
- **T-LSTM** [4] is a time-aware Long-Short Term Memory (LSTM) model with memory decomposition for irregular time series classification. We modify it to predict traffic states using a LSTM-based decoder.
- **DCRNN** [18] is a representative approach based on GNNs and RNNs for typical traffic forecasting tasks, which replaces the matrix multiplications in GRU with a graph convolution operation. The used graph structure is the same as ASEER, and the diffusion step is set to 1. To apply DCRNN to our problem, we pad the input traffic sequences of all nodes to the same length.

- **GWNet** [33] is a representative approach based on GNNs and CNNs for typical traffic forecasting. It stacks multiple spatial-temporal blocks that are constructed by the graph convolution layer and gated TCN layer, where the graph convolution is performed on the combination of pre-defined and self-learned adjacency matrix. The pre-defined graph structure is the same as ASEER. We stack 3 blocks with 4 convolution layers, and set convolution filter size to 3. It adopts the same padding strategy with DCRNN.
- **mTAND** [27] is a state-of-the-art transformer-based approach for irregularly sampled multivariate time series classification and interpolation tasks. It adopts multi-time attention with time embedding to produce a fixed-length representation of a variable-length time series. The reference point number is set to 64.

4.5 Overall Performance

Table 2 reports the overall performance of ASEER and all compared baselines on two datasets *w.r.t.* six metrics. As can be seen, ASEER achieves the best overall performance among all the compared approaches on two datasets, which demonstrates our model’s superiority in irregular traffic forecasting task. Besides, we have several observations. Firstly, all learnable approaches outperform the statistical approaches (*i.e.*, LAST, HA), which validates that the data-driven approaches to learn complex non-linear interactions within traffic data is helpful for our task. Secondly, we find CNN-based baselines TCN and GWNet do not achieve a desired performance for the reason that typical CNN applies the same parameterized filters to process sequences with different time intervals, which is incompetent to model the temporal dependency in such irregular sequences. Thirdly, we observe ASEER obtains a superior overall performance than approaches (*i.e.*, GRU-D, T-LSTM, and mTAND) for irregular time series, as these approaches fail to model spatial dependencies within traffic data. From these approaches, we notice mTAND has a slight advantage in C-MAPE than ASEER on ZHUZHOU. This is probably because mTAND as a powerful approach for interpolation task performs well in the short-term future cycles’ beginning times prediction. However, ASEER significantly outperforms mTAND in the other metrics. Lastly, we observe a notable performance improvement by comparing ASEER with GNNs-based approaches (*i.e.*, DCRNN and GWNet) for typical

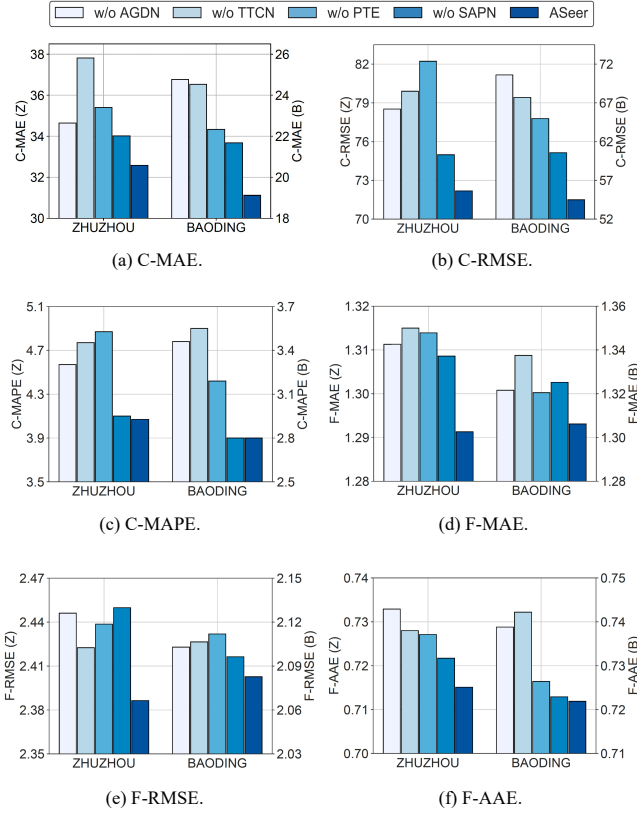


Figure 8: Results of ablation study. "Z" and "B" denote ZHUZHOU and BAODING, respectively.

traffic forecasting. The improvement can be majorly attributed to that ASEer enables to model asynchronous spatial dependency and irregular temporal dependency in our task.

4.6 Ablation Study

We evaluate the performance of ASEer and its four variants on both ZHUZHOU and BAODING in all six metrics. (1) **w/o AGDN** removes the AGDN module; (2) **w/o TTCN** replaces TTCN with a 1D CNN, whose filter size is set to the maximal sequence length in the dataset; (3) **w/o PTE** removes personalized time encoding; (4) **w/o SAPN** replaces SAPN with an autoregressive MLP predictor. The results of ablation study are shown in Figure 8. As can be seen, removing any component causes notable overall performance degradation compared to ASEer, which demonstrates the effectiveness of each component. From these results, we observe **w/o TTCN** almost results in significant performance descent for all metrics on both datasets, which verifies the effectiveness of TTCN to improve typical CNN to model the temporal dependency within irregular traffic sequences. In addition, **w/o AGDN** causes a remarkable accuracy decline for all the metrics *w.r.t.* traffic flow, which validates the effect of AGDN on modeling asynchronous spatial dependency of traffic dynamics. We also observe **w/o AGDN** causes a more obvious accuracy decline on BAODING than ZHUZHOU for three

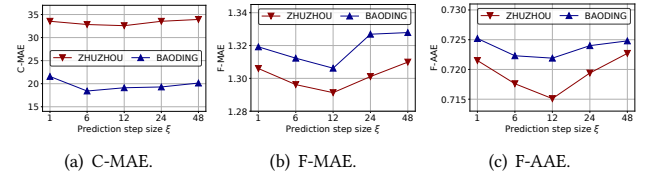


Figure 9: Effect of different prediction step sizes.

metrics *w.r.t.* cycle lengths. This is probably because the distribution of cycle lengths in BAODING is denser, AGDN's smoothness induces a more precise prediction. Moreover, we notice that **w/o PTE** leads to a consistent performance reduction for all metrics on both datasets, which demonstrates that a well-learned personalized time encoding function to embed continuous time for each lane can facilitate the prediction of both cycle lengths and traffic flows. Finally, by comparing ASEer with **w/o SAPN**, we observe a more obvious performance degradation on BAODING for metrics *w.r.t.* cycle lengths, which is probably because the sequence is longer on BAODING, an autoregressive model causes a severe error accumulation problem on cycle length prediction. **w/o SAPN** also shows a consistent performance descent for three metrics *w.r.t.* traffic flow, which confirms that SAPN indeed improves the long cycle length and traffic flow sequence prediction performance.

4.7 Parameter Sensitivity

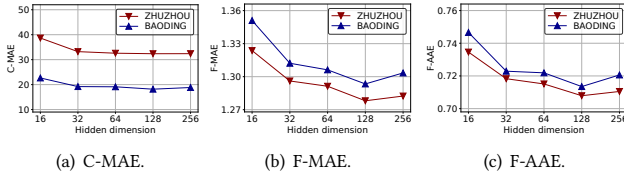
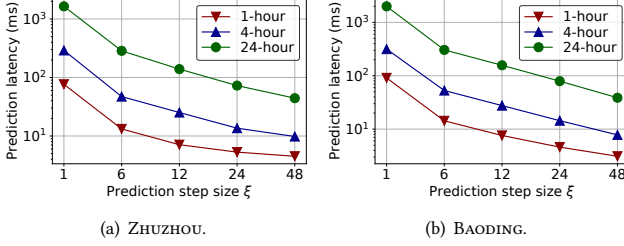
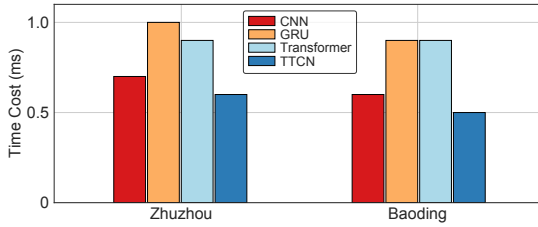
We conduct experiments for two important hyper-parameters, *i.e.*, the prediction step size ξ and dimension of all hidden layers, on both ZHUZHOU and BAODING to study the sensitivity of these hyper-parameters. We report experimental results on metrics C-MAE, F-MAE, and F-AAE to evaluate the model's prediction performance on both cycle lengths and traffic flows.

Figure 9 shows the results of varying the prediction step size ξ from 1 to 48. As can be seen, there is a notable overall prediction performance improvement by increasing ξ from 1 (autoregressive model) to 12 (semi-autoregressive model), which demonstrates the effectiveness of SAPN to mitigate error accumulation problem in the autoregressive prediction model. However, we also observe a performance degradation when the prediction step size is too large. This is probably because a too-large prediction step size may result in under-training for SAPN to make predictions based on different elapsed times.

We vary the dimension of model's all hidden layers from 16 to 256. The results are shown in Figure 10. We can observe a remarkable prediction performance improvement by increasing the hidden dimension from 16 to 32, and the performance is continuously improving and achieves the best when the dimension is set to 128. However, a larger hidden dimension also takes more expensive computational overhead. Thus, we have to balance the performance and computation cost for the selection of model's hidden dimension.

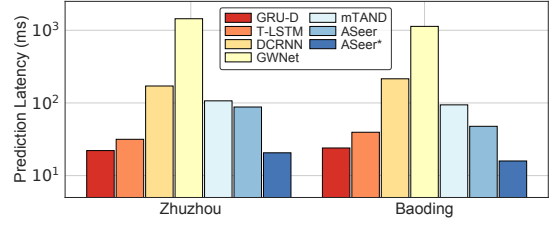
4.8 Prediction Efficiency Analysis

We conduct experiments to test the prediction efficiency of different models. To ensure a fair comparison, we eliminate the influence of different models on the prediction lengths by standardizing the


Figure 10: Effect of different hidden dimensions.

Figure 11: Prediction latency of SAPN with different prediction step sizes.

Figure 12: Efficiency of different modules in temporal modeling.

prediction process. This involves allowing all models to predict the maximum lengths of the corresponding ground truth sequences.

4.8.1 Efficiency of SAPN. To evaluate the effect of SAPN on prediction efficiency, we conduct experiments on both ZHUZHOU and BAODING to specifically test SAPN’s average prediction latency based on different prediction step sizes ξ from 1 to 48. We report the respective results of predicting future 1, 4, and 24 hours traffic states in Figure 11. As can be seen, the prediction latency is notably reduced by comparing semi-autoregressive models ($\xi > 1$) with autoregressive model ($\xi = 1$) due to the reduction of total prediction steps. The magnitude of latency reduction even approaches the prediction step size when we predict longer sequences or the step size is not too large, which demonstrates the significant effectiveness of SAPN to improve prediction efficiency. We also observe with the prediction step size increasing, the prediction latency is consistently reduced, and with the predicted hours rising, the model can have a significantly higher prediction efficiency by setting a larger prediction step size. This observation indicates that we can choose a larger prediction step size with the predicted sequence length increasing for higher prediction efficiency.


Figure 13: Efficiency comparison between different models.

4.8.2 Efficiency of TTCN. To study TTCN’s efficiency, we replace TTCN with several commonly used modules in temporal modeling, *i.e.*, CNN, GRU, and Transformer, and test their running time costs. As illustrated in Figure 12, TTCN achieves more than 40% and 33% faster results than GRU and transformer, respectively, on both datasets. Furthermore, to our surprise, TTCN exhibits even faster than CNN. This is probably because TTCN can directly handle variable-length sequences with transformable filter sizes, while CNN is limited to processing fixed-length sequences via padding or clipping, thus it may cost additional time to process longer sequences beyond their original lengths. All the observations demonstrate the efficiency of TTCN.

4.8.3 Efficiency Comparison. Figure 13 displays the comparison of average prediction latency between ASEER and other state-of-the-art baseline models, where GRU-D, T-LSTM, and DCRNN are autoregressive models. To enable GWNNet and mTAND to predict the variable-length sequence, we let them perform in an autoregressive way. We can observe ASEER (87.9ms, 47.7ms with $\xi = 12$) is markedly more efficient than the other graph-based baselines, *i.e.*, DCRNN (171.1ms, 214.9ms) and GWNNet (1441.4ms, 1131.4ms) on both ZHUZHOU and BAODING. Moreover, by restricting the usage of buffer messages $K = 10$ in Eq. (22), ASEER* can achieve the fastest prediction latency (20.6ms, 15.9ms) compared to all these state-of-the-art models without losing too much prediction accuracy (in Table 3). The results verify our model’s efficiency in practical real-time traffic forecasting applications. The efficiency of ASEER is mainly attributed to three reasons: (1) SAPN is much more efficient than a fully autoregressive model; (2) TTCN can be efficiently computed in parallel like CNN; and (3) AGDN enables pre-computation of spatial representations in advance, allowing them to be readily available for responding to real-time traffic forecasting requests.

5 RELATED WORK

5.1 Traffic Forecasting

Recently years, deep learning models have dominated the traffic forecasting tasks for their extraordinary capability in modeling the complex spatio-temporal characteristics of traffic data [2, 9, 11, 15, 18, 26, 33–36, 41]. In spatial modeling, a part of studies [34, 36] first partition a city into a grid-based region map, then utilize Convolutional Neural Networks (CNNs) to capture spatial dependencies between adjacent regions. After that, Graph Neural Networks (GNNs) [8, 14, 30, 32] are widely used to model the non-euclidean spatial dependencies in traffic data [13, 20, 26]. For example, studies [18, 35] employ GNNs to model the traffic flow

Table 3: Variation of prediction performance and latency by restricting messages usage in the buffer. ASEER* denotes ASEER with a restriction $K = 10$.

Dataset	Algorithm	C-MAE	C-RMSE	C-MAPE	F-MAE	F-RMSE	F-AAE	Latency
ZHUZHOU	ASEER	32.5803	72.1835	4.10%	1.2913	2.3864	0.7151	87.9ms
	ASEER*	32.8299	72.7056	4.13%	1.2939	2.3954	0.7166	20.6ms
BAODING	ASEER	19.1188	54.4919	2.80%	1.3062	2.0827	0.7219	47.7ms
	ASEER*	19.3724	55.1685	2.84%	1.3078	2.0871	0.7232	15.9ms

diffusion process in the road network. Studies [11, 37, 41] incorporate attention mechanism into GNNs to learn the dynamic spatial dependencies between the road network sensors. In addition to the pre-defined relational graph derived from road networks, some works [2, 15, 33] attempt to directly learn the latent graph structure from traffic data. In temporal modeling, CNNs [11, 15, 33, 35, 36] and Recurrent Neural Networks (RNNs) [2, 18, 34] are frequently adopted to capture temporal dependencies within traffic data. Compared to RNNs in temporal modeling, CNNs enable the parallel computing for all time steps, which exhibits extreme advantages in computational efficiency. However, all the methods of above studies are designed for the time-aligned traffic data with fixed time interval, *a.k.a.* raster data [1], which fails to handle the challenges of asynchronous spatial dependency and irregular temporal dependency in our irregular traffic forecasting problem.

5.2 Irregularly Sampled Time Series

This work is also related to the literature about learning from irregularly sampled time series, which is a kind of time series data characterized by varying time intervals between temporally adjacent observations [40]. A straightforward approach is to divide the irregularly sampled time series into a regular one with fixed time intervals [19]. However, such a temporal discretization method may lead to information loss and data missing problems [27, 28]. Recent studies tend to directly learn from irregularly sampled time series. Specifically, some studies improve RNNs by using a time gate [23], a time decay term [5], or memory decomposition mechanism [4] to adjust RNNs’ memory update for sequences with irregular time intervals. Another line of studies introduce Neural Ordinary Differential Equations (NODEs) [6] to model the continuous dynamics in time series, and assume the latent states of time series are continuously evolving through continuous time [24, 25]. However, it is unreasonable to directly apply NODEs to model the continuous dynamics of traffic flow since it is defined over a period of time instead of a time point. Besides, attention mechanism is also applied to model irregularly sampled time series. For example, Horn et al. [12] directly employs an attention mechanism to summarize all the observations of irregularly sampled multivariate time series. Shukla and Marlin [27] proposes a multi-time attention network to learn embedding of continuous time. Zhang et al. [40] introduce a GNN to capture time-varying dependencies between sensors by performing the graph convolution operation at all timestamps when there is an observation at an arbitrary sensor. However, it will be extremely time-consuming once the data is significantly asynchronous among large-scale sensors like us. Moreover, it targets solving a multivariate time series classification task. Ultimately, to our knowledge,

there are no prior studies attempting to modify CNNs to adapt to the irregular time series modeling.

6 CONCLUSION

In this paper, we investigated a new irregular traffic forecasting problem which aims to predict traffic state sequences for the lanes entering intelligent intersections in a future time window, and presented an Asynchronous Spatio-Temporal Graph Convolutional Network, ASEER, to address this problem. Specifically, by representing lanes as nodes and linking them via a traffic diffusion graph, we first proposed an Asynchronous Graph Diffusion Network to model the asynchronous spatial dependency between the time-misaligned traffic state measurements of nodes. After that, to capture the temporal dependency within irregular traffic state sequences, we devised a personalized time encoding to embed the continuous time for each node and proposed a Transformable Time-aware Convolution Network to perform efficient temporal convolution on irregular traffic sequences. Furthermore, a Semi-Autoregressive Prediction Network was further designed to iteratively predict variable-length traffic state sequences in an effective and efficient way. Finally, extensive experiments on two real-world datasets demonstrated the effectiveness of ASEER compared with nine competitive baseline algorithms in six metrics.

REFERENCES

- [1] Gowtham Atluri, Anuj Karpatne, and Vipin Kumar. 2018. Spatio-temporal data mining: A survey of problems and methods. *ACM Computing Surveys (CSUR)* (2018), 1–41.
- [2] Lei Bai, Lina Yao, Can Li, Xianzhi Wang, and Can Wang. 2020. Adaptive graph convolutional recurrent network for traffic forecasting. *Advances in neural information processing systems* 33 (2020), 17804–17815.
- [3] Shaojie Bai, J Zico Kolter, and Vladlen Koltun. 2018. An empirical evaluation of generic convolutional and recurrent networks for sequence modeling. *arXiv preprint arXiv:1803.01271* (2018).
- [4] Inci M Baytas, Cao Xiao, Xi Zhang, Fei Wang, Anil K Jain, and Jiayu Zhou. 2017. Patient subtyping via time-aware LSTM networks. In *Proceedings of the 23rd ACM SIGKDD international conference on knowledge discovery and data mining*. 65–74.
- [5] Z Che, S Purushotham, K Cho, D Sontag, and Y Liu. 2018. Recurrent Neural Networks for Multivariate Time Series with Missing Values. *Scientific reports* (2018), 6085–6085.
- [6] Ricky TQ Chen, Yulia Rubanova, Jesse Bettencourt, and David Duvenaud. 2018. Neural ordinary differential equations. In *Proceedings of the 32nd International Conference on Neural Information Processing Systems*. 6572–6583.
- [7] Junyoung Chung, Caglar Gulcehre, Kyunghyun Cho, and Yoshua Bengio. 2014. Empirical evaluation of gated recurrent neural networks on sequence modeling. In *NIPS Workshop on Deep Learning*.
- [8] Michaël Defferrard, Xavier Bresson, and Pierre Vandergheynst. 2016. Convolutional neural networks on graphs with fast localized spectral filtering. *Advances in neural information processing systems* (2016), 3844–3852.
- [9] Zheng Fang, Qingqing Long, Guojie Song, and Kunqing Xie. 2021. Spatial-temporal graph ode networks for traffic flow forecasting. In *Proceedings of the 27th ACM SIGKDD conference on knowledge discovery & data mining*. 364–373.
- [10] Qiangqiang Guo, Li Li, and Xuegang Jeff Ban. 2019. Urban traffic signal control with connected and automated vehicles: A survey. *Transportation research part C: emerging technologies* (2019), 313–334.

- [11] Shengnan Guo, Youfang Lin, Ning Feng, Chao Song, and Huaiyu Wan. 2019. Attention based spatial-temporal graph convolutional networks for traffic flow forecasting. In *Proceedings of the AAAI conference on artificial intelligence*. 922–929.
- [12] Max Horn, Michael Moor, Christian Bock, Bastian Rieck, and Karsten Borgwardt. 2020. Set functions for time series. In *International Conference on Machine Learning*. PMLR, 4353–4363.
- [13] Weiwei Jiang and Jiayun Luo. 2022. Graph neural network for traffic forecasting: A survey. *Expert Systems with Applications* (2022), 117921.
- [14] Thomas N. Kipf and Max Welling. 2017. Semi-Supervised Classification with Graph Convolutional Networks. In *International Conference on Learning Representations, ICLR*.
- [15] Shiyong Lan, Yitong Ma, Weikang Huang, Wenwu Wang, Hongyu Yang, and Pyang Li. 2022. Dstagnn: Dynamic spatial-temporal aware graph neural network for traffic flow forecasting. In *International Conference on Machine Learning*. PMLR, 11906–11917.
- [16] Yann LeCun, Yoshua Bengio, and Geoffrey Hinton. 2015. Deep learning. *nature* (2015), 436–444.
- [17] Yuying Li and Qipeng Liu. 2020. Intersection management for autonomous vehicles with vehicle-to-infrastructure communication. *PLoS one* (2020), e0235644.
- [18] Yaguang Li, Rose Yu, Cyrus Shahabi, and Yan Liu. 2018. Diffusion Convolutional Recurrent Neural Network: Data-Driven Traffic Forecasting. In *International Conference on Learning Representations*.
- [19] Zachary C Lipton, David Kale, and Randall Wetzel. 2016. Directly modeling missing data in sequences with rnns: Improved classification of clinical time series. In *Machine learning for healthcare conference*. PMLR, 253–270.
- [20] Hao Liu, Jindong Han, Yanjie Fu, Jingbo Zhou, Xinjiang Lu, and Hui Xiong. 2020. Multi-modal transportation recommendation with unified route representation learning. *Proceedings of the VLDB Endowment* (2020), 342–350.
- [21] Ivan Marisca, Andrea Cini, and Cesare Alippi. 2022. Learning to Reconstruct Missing Data from Spatiotemporal Graphs with Sparse Observations. In *Advances in Neural Information Processing Systems*.
- [22] Fernando Moreno-Pino, Pablo M Olmos, and Antonio Artés-Rodríguez. 2023. Deep autoregressive models with spectral attention. *Pattern Recognition* (2023), 109014.
- [23] Daniel Neil, Michael Pfeiffer, and Shih-Chii Liu. 2016. Phased LSTM: accelerating recurrent network training for long or event-based sequences. In *Proceedings of the 30th International Conference on Neural Information Processing Systems*. 3889–3897.
- [24] Yulia Rubanova, Ricky TQ Chen, and David Duvenaud. 2019. Latent ODEs for irregularly-sampled time series. In *Proceedings of the 33rd International Conference on Neural Information Processing Systems*. 5320–5330.
- [25] Mona Schirmer, Mazin Eltayeb, Stefan Lessmann, and Maja Rudolph. 2022. Modeling irregular time series with continuous recurrent units. In *International Conference on Machine Learning*. PMLR, 19388–19405.
- [26] Zezhi Shao, Zhao Zhang, Wei Wei, Fei Wang, Yongjun Xu, Xin Cao, and Christian S Jensen. 2022. Decoupled dynamic spatial-temporal graph neural network for traffic forecasting. *Proceedings of the VLDB Endowment* (2022), 2733–2746.
- [27] Satya Narayan Shukla and Benjamin Marlin. 2021. Multi-Time Attention Networks for Irregularly Sampled Time Series. In *International Conference on Learning Representations*.
- [28] Satya Narayan Shukla and Benjamin M Marlin. 2020. A survey on principles, models and methods for learning from irregularly sampled time series. *arXiv preprint arXiv:2012.00168* (2020).
- [29] Ashish Vaswani, Noam Shazeer, Niki Parmar, Jakob Uszkoreit, Llion Jones, Aidan N Gomez, Lukasz Kaiser, and Illia Polosukhin. 2017. Attention is all you need. *Advances in neural information processing systems* 30 (2017).
- [30] Petar Veličković, Guillem Cucurull, Arantxa Casanova, Adriana Romero, Pietro Liò, and Yoshua Bengio. 2018. Graph Attention Networks. In *International Conference on Learning Representations*.
- [31] Hua Wei, Guanjie Zheng, Vikash Gayah, and Zhenhui Li. 2019. A survey on traffic signal control methods. *arXiv preprint arXiv:1904.08117* (2019).
- [32] Zonghan Wu, Shirui Pan, Fengwen Chen, Guodong Long, Chengqi Zhang, and S Yu Philip. 2020. A comprehensive survey on graph neural networks. *IEEE transactions on neural networks and learning systems* (2020), 4–24.
- [33] Zonghan Wu, Shirui Pan, Guodong Long, Jing Jiang, and Chengqi Zhang. 2019. Graph wavenet for deep spatial-temporal graph modeling. In *Proceedings of the International Joint Conference on Artificial Intelligence*. 1907–1913.
- [34] Huaxiu Yao, Fei Wu, Jintao Ke, Xianfeng Tang, Yitian Jia, Siyu Lu, Pinghua Gong, Zhenhui Li, Jieping Ye, and Didi Chuxing. 2018. Deep multi-view spatial-temporal network for taxi demand prediction. In *Proceedings of the AAAI conference on artificial intelligence*. AAAI press, 2588–2595.
- [35] Bing Yu, Hao Teng Yin, and Zhanxing Zhu. 2018. Spatio-temporal graph convolutional networks: a deep learning framework for traffic forecasting. In *Proceedings of the 27th International Joint Conference on Artificial Intelligence*. 3634–3640.
- [36] Junbo Zhang, Yu Zheng, and Dekang Qi. 2017. Deep spatio-temporal residual networks for citywide crowd flows prediction. In *Proceedings of the AAAI conference on artificial intelligence*. 1655–1661.
- [37] Weijia Zhang, Hao Liu, Yanchi Liu, Jingbo Zhou, and Hui Xiong. 2020. Semi-supervised hierarchical recurrent graph neural network for city-wide parking availability prediction. In *Proceedings of the AAAI Conference on Artificial Intelligence*. 1186–1193.
- [38] Weijia Zhang, Hao Liu, Fan Wang, Tong Xu, Haoran Xin, Dejing Dou, and Hui Xiong. 2021. Intelligent electric vehicle charging recommendation based on multi-agent reinforcement learning. In *Proceedings of the Web Conference 2021*. 1856–1867.
- [39] Weijia Zhang, Hao Liu, Lijun Zha, Hengshu Zhu, Ji Liu, Dejing Dou, and Hui Xiong. 2021. MugRep: A multi-task hierarchical graph representation learning framework for real estate appraisal. In *Proceedings of the 27th ACM SIGKDD conference on knowledge discovery and data mining*. 3937–3947.
- [40] Xiang Zhang, Marko Zeman, Theodoros Tsiligkaridis, and Marinka Zitnik. 2022. Graph-Guided Network for Irregularly Sampled Multivariate Time Series. In *International Conference on Learning Representations*.
- [41] Chuanpan Zheng, Xiaoliang Fan, Cheng Wang, and Jianzhong Qi. 2020. Gman: A graph multi-attention network for traffic prediction. In *Proceedings of the AAAI conference on artificial intelligence*. 1234–1241.